Shear transport in far-from-equilibrium isotropization of supersymmetric Yang-Mills plasma

Shoucheng Wang

Institute of Theoretical Physics, Chinese Academy of Sciences

December 4, 2024

Based on arXiv: 2411.10706, in collaboration with Prof. Li Li, Song He

1. Introduction
2. Holographic Setup
3. Far-from-equilibrium isotropization
4. Shear flows in far-from-equilibrium isotropization dynamics
5. Conclusions

Introduction

- The isotropization of non-equilibrium states in QCD and other non-Abelian quantum field theories has become a pivotal topic due to its broad relevance in heavy-ion collisions, early universe cosmology, and other domains.
- A key challenge lies in comprehending the rapid isotropization time of the QGP. Perturbative methods have not provided a quantitative framework for studying such strongly coupled processes, motivating the exploration of thermalization in strongly coupled media through the holographic approach.
- A proper toy model for studying the dynamics of a far-from-equilibrium, strongly coupled non-Abelian plasma in a controlled setting is strongly coupled $\mathcal{N}=4$ supersymmetric Yang-Mills theory.

c	1	1.5	2	2.5	3	3.5	4
τ_{iso}/τ	3	2.2	1.7	1.8	1.8	1.9	1.9

Result from Chesler et al. PRL 102, 211601 (2009). c denotes the strength of quench, $\tau = 1$. $\tau_{iso}/\tau = 1.7$ corresponds to 0.5 fm$/c$ while $T = 350$ Mev.

Introduction

- Despite extensive research on isotropization dynamics in the holographic literature, shear viscosity in far-from-equilibrium isotropization has not yet been thoroughly explored.
- For strongly interacting quantum field theories that admit gravity duals, holographic computations using linear response theory (the Kubo formula) have led to a conjectured viscosity bound, known as the Kovtun-Son-Starinets (KSS) bound $\eta_0/\mathcal{S} = 1/4\pi \approx 0.80$. PRL 94, 111601 (2005)
- Hower, the shear viscosity far from equilibrium might display much richer dynamics than its near-equilibrium counterpart when directly compute the time-dependent boundary stress tensor, which is a nonlinear function of the shear rate.

The dual five-dimensional gravitational theory,

$$S = \frac{1}{2\kappa_N^2} \int d^5x \sqrt{-g} \left[\mathcal{R} + \frac{12}{L^2} \right] , \tag{1}$$

The background metric $g_{\mu\nu}^B(x)$, PRL 102, 211601 (2009)

$$ds^2 = -dt^2 + e^{B_0(t)} d\mathbf{x}_\perp^2 + e^{-2B_0(t)} dx_\parallel^2 , \tag{2}$$

The function $B_0(t)$ is chosen to be

$$B_0(t) = \frac{1}{2} c \left[1 - \tanh\left(\frac{t}{\tau}\right) \right] , \tag{3}$$

The corresponding bulk configuration is given as follows.

$$ds^2 = -A(t,r)\, dt^2 + \Sigma(t,r)^2 \left[e^{B(t,r)} d\mathbf{x}_\perp^2 + e^{-2B(t,r)} dx_\parallel^2 \right] + 2\, dr dt , \tag{4}$$

The functions (A, B, Σ) are determined by solving the Einstein's equations

$$\mathcal{R}_{\mu\nu} - \frac{1}{2}\mathcal{R} g_{\mu\nu} - 6 g_{\mu\nu} = 0\,, \tag{5}$$

with the explicit form of equations of motion given as

$$0 = \Sigma'' + \frac{1}{2}\Sigma B'^2\,, \tag{6a}$$

$$0 = d_+\Sigma' - 2\Sigma + \frac{2}{\Sigma} d_+\Sigma\Sigma'\,, \tag{6b}$$

$$0 = d_+B' + \frac{3}{2\Sigma} d_+B\Sigma' + \frac{3}{2\Sigma} d_+\Sigma B'\,, \tag{6c}$$

$$0 = A'' + 4 + 3 d_+B B' - \frac{12}{\Sigma^2} d_+\Sigma\Sigma'\,, \tag{6d}$$

$$0 = d_+(d_+\Sigma) + \frac{1}{2} d_+B^2\Sigma - \frac{1}{2} d_+\Sigma A'\,, \tag{6e}$$

For any function $f(r, t)$ we have defined

$$f' \equiv \partial_r f\,, \quad \dot{f} \equiv \partial_t f\,, \quad d_+ f \equiv \partial_t f + \frac{1}{2} A \partial_r f\,, \tag{7}$$

Near the AdS boundary, we have the following asymptotic expansion.

$$\begin{aligned} A(r,t) &= r^2 - \frac{5}{4}\dot{B}_0(t)^2 + \frac{a_4(t)}{r^2} + \frac{\ln(r)\left(-3\dot{B}_0(t)^4 + 2\dddot{B}_0(t)\dot{B}_0(t) - \ddot{B}_0(t)^2\right)}{8r^2} + \mathcal{O}\left(\frac{\ln(r)}{r^3}\right), \\ \Sigma(r,t) &= r - \frac{\dot{B}_0(t)^2}{4r} - \frac{\dot{B}_0(t)\ddot{B}_0(t)}{12r^2} + \mathcal{O}\left(\frac{\ln(r)}{r^3}\right), \\ B(r,t) &= B_0(t) + \frac{\dot{B}_0(t)}{r} + \frac{\ddot{B}_0(t)}{4r^2} + \frac{-\dddot{B}_0(t) + 5\dot{B}_0(t)^3}{12r^3} + \frac{b_4(t)}{r^4} \\ &\quad + \frac{\ln(r)}{16r^4}\left(\ddddot{B}_0(t) - 6\dot{B}_0(t)^2\ddot{B}_0(t)\right) + \mathcal{O}\left(\frac{\ln(r)}{r^5}\right), \end{aligned} \tag{8}$$

together with a constraint relation

$$\dot{a}_4(t) = 4b_4(t)\dot{B}_0(t) + \frac{17}{48}\dot{B}_0(t)\ddddot{B}_0(t) - \frac{5}{2}\dot{B}_0(t)^3\ddot{B}_0(t) - \frac{1}{8}\dddot{B}_0(t)\ddot{B}_0(t)\,. \tag{9}$$

The stress tensor of the supersymmetric Yang-Mills theory can be obtained by holographic renormalization. One has

$$T^{\mu}{}_{\nu} = \mathrm{diag}(-\mathcal{E}, \mathcal{P}_{\perp}, \mathcal{P}_{\perp}, \mathcal{P}_{\|}) \,, \tag{10}$$

with

$$\kappa_N^2 \mathcal{E} = -\frac{3}{2} a_4(t) - \frac{1}{128}\left(14\ddot{B}_0(t)^2 + 3\dot{B}_0(t)^4 - 4\dddot{B}_0(t)\dot{B}_0(t)\right) , \tag{11}$$

$$\begin{aligned} \kappa_N^2 \mathcal{P}_{\perp} = -\frac{1}{2} a_4(t) + 2b_4(t) + \frac{1}{384}\Big(&64\ddddot{B}_0(t) + 10\ddot{B}_0(t)^2 + 21\dot{B}_0(t)^4 + 4\dddot{B}_0(t)\dot{B}_0(t) \\ &-468\dot{B}_0(t)^2\ddot{B}_0(t)\Big) , \end{aligned} \tag{12}$$

$$\begin{aligned} \kappa_N^2 \mathcal{P}_{\|} = -\frac{1}{2} a_4(t) - 4b_4(t) + \frac{1}{384}\Big(&-128\ddddot{B}_0(t) + 10\ddot{B}_0(t)^2 + 21\dot{B}_0(t)^4 + 4\dddot{B}_0(t)\dot{B}_0(t) \\ &+936\dot{B}_0(t)^2\ddot{B}_0(t)\Big) . \end{aligned} \tag{13}$$

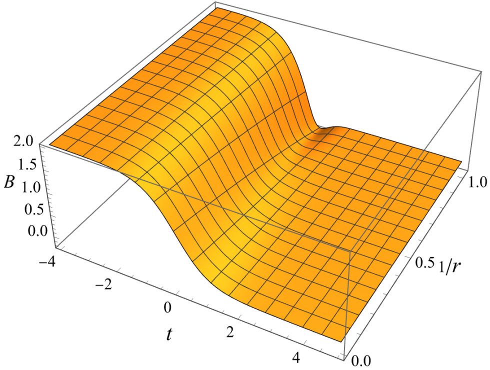

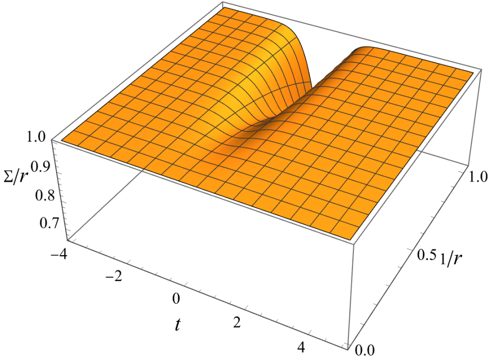

Illustration of the bulk configuration $(B, \Sigma/r)$ during far-from-equilibrium isotropization for $c = 2$. In our coordinate system, the AdS boundary is located at $r \to \infty$ at which $B = B_0(t)$ is a boundary condition. Near $t = 0$, the geometry exhibits significant anisotropy due to the quenching effect via (3).

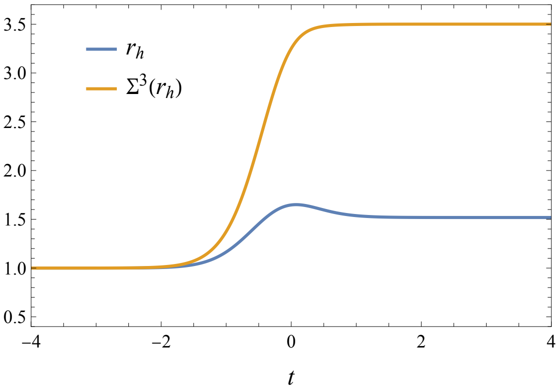

The evolution of the location of the apparent horizon r_h and the apparent horizon area $\Sigma^3(r_h)$.
The area of the apparent horizon increases monotonically as time evolves.

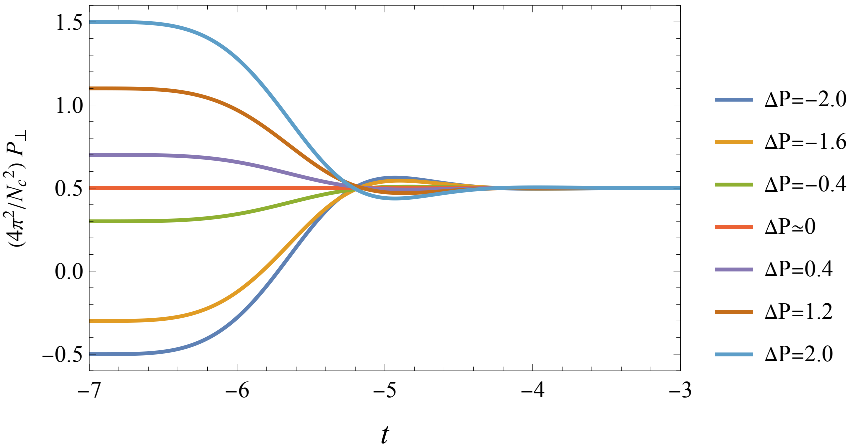

Transverse pressure $(P_\perp)$ for various initial pressure anisotropy $\Delta P = \frac{P_\perp(t_0) - P_\parallel(t_0)}{\mathcal{E}(t_0)}$ with the same initial energy density. The pressure anisotropy increases as $b_4(t_0)$ is increased. We choose $a_4(t_0) = -1$ with $t_0 = -7$ and $c = 2$ for the dynamic boundary (3).

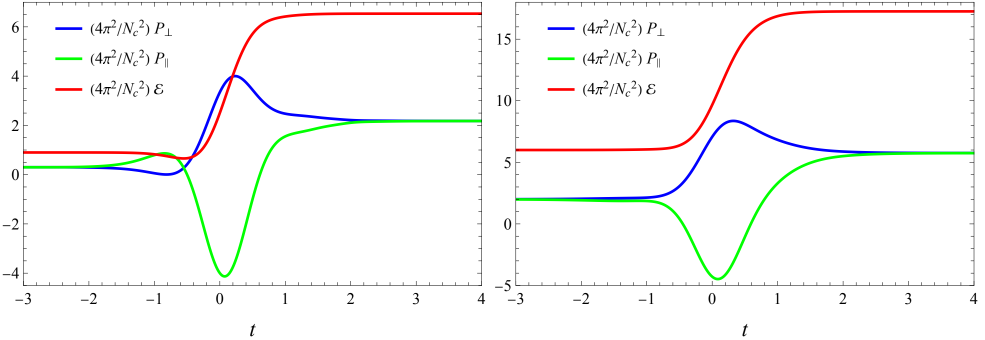

Time evolution of energy density $\mathcal{E}$, transverse pressure ($P_\perp$), and longitudinal pressure ($P_\parallel$) for $c = 2$. Left panel corresponds to a small initial energy density ($a_4(t_0) = -0.6$) and right panel has a large one ($a_4(t_0) = -4$). Following a brief period of anisotropic geometry, all quantities converge to equilibrium late. It is manifest that the energy density appears to be driven below the ground state energy density in the first moments of the quench.

- The isotropization time, $\tau_{\rm iso}$, is defined as the time at which both transverse and longitudinal pressures reach within 10% of their final equilibrium values.
- The thermal equilibrium state at late times is given by

$$T^{\mu\nu}_{eq} = \frac{\pi^2 N_c^2 T_{eq}^4}{8}\text{diag}(3,1,1,1)\,, \tag{14}$$

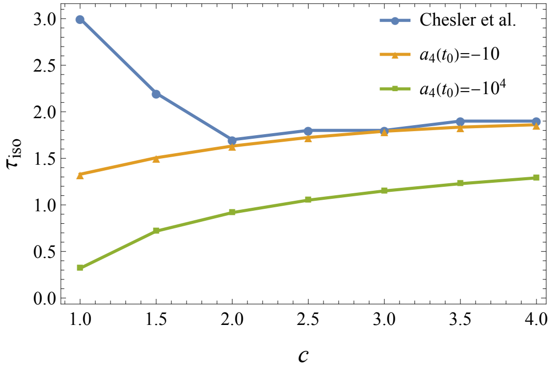

Isotropization time as a function of quench strength c for different initial data. Our results are compared with the isotropization time from Chesler et al. (2008) where $a_4(t_0) \approx 0$. The large initial energy densities accelerate the isotropization significantly.

According to arXiv:2109.11701, we derive the viscosity coefficient η corresponding the boundary metric (3) as

$$\eta = \frac{\mathcal{P}_\parallel - \mathcal{P}_\perp}{3\dot{B}_0(t)} \tag{15}$$

$\dot{B}_0(t)$ acts as the shear rate. Using the constraint equation (9),

$$\dot{\mathcal{E}}(t) = 3\eta\,\dot{B}_0(t)^2 \,. \tag{16}$$

Then by performing a coordinate transformation

$$\begin{aligned} x &= \frac{1}{\sqrt{6}}(-\sqrt{3}x_1 - x_2 + \sqrt{2}x_\parallel)\,, \\ y &= \frac{1}{\sqrt{3}}(\sqrt{2}x_2 + x_\parallel)\,, \\ z &= \frac{1}{\sqrt{6}}(\sqrt{3}x_1 - x_2 + \sqrt{2}x_\parallel)\,, \end{aligned} \tag{17}$$

we have

$$\pi'^{\mu}{}_{\nu} = \begin{bmatrix} 0 & \sigma & \sigma \\ \sigma & 0 & \sigma \\ \sigma & \sigma & 0 \end{bmatrix}, \quad \sigma'^{\mu}{}_{\nu} = -\frac{\dot{B}_0}{2}\begin{bmatrix} 0 & 1 & 1 \\ 1 & 0 & 1 \\ 1 & 1 & 0 \end{bmatrix}, \quad \sigma = \eta\,\dot{B}_0 \tag{18}$$

shear deformations are carried out with the same shear rate, $\dot{B}_0$, in all three spatial directions.

The entropy density is associated with the area element of the apparent horizon

$$\mathcal{S}(t) = \frac{2\pi\Sigma(t, r_h)^3}{\kappa_N^2}, \qquad (19)$$

the entropy production is given by

$$\nabla_\mu s^\mu = \frac{2\pi}{\kappa_N^2}\frac{\partial}{\partial t}\Sigma(t, r_h)^3, \qquad (20)$$

where $s^\mu = \mathcal{S}u^\mu$ denotes the entropy current density. We find that the entropy production (20) is always positive in all cases we consider.

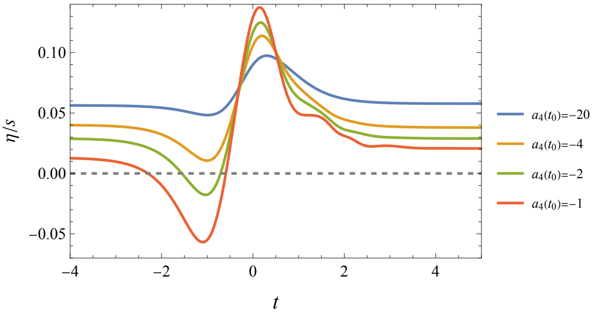

Shear viscosity to entropy density ratio, $\eta/\mathcal{S}$, in far-from-equilibrium isotropization with $c = 2$. The lines with different colors correspond to different initial energy densities set by $a_4(t_0)$.

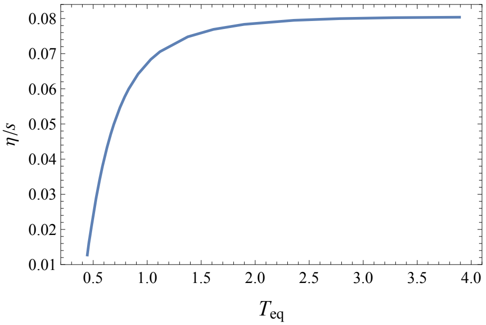

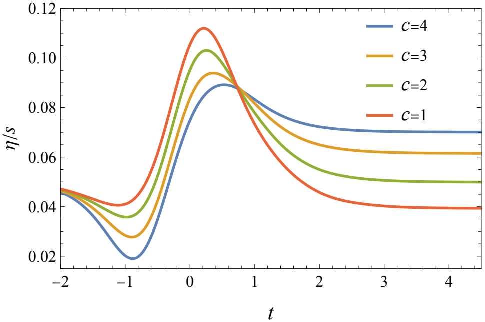

Left: The late time equilibrium $\eta/\mathcal{S}$ as a function of the equilibrium temperature T_{eq} for $c = 2$. It approaches $1/4\pi$ from below as the temperature is increased. **Right**: The evolution of $\eta/\mathcal{S}$ during far-from-equilibrium isotropization for different values of c with the same initial data.

For the shear function (3), there are two required conditions in the limit $t \to \infty$ to make the viscosity-to-entropy ratio, $\eta/\mathcal{S}$, equal to the KSS bound, $\eta_0/\mathcal{S} = 1/4\pi \approx 0.80$,

$$\dot{B}_0 \tau_c \ll 1\,, \tag{21}$$

$$\tau_c^{n-1} \partial_t^n B_0 \ll \dot{B}_0\,. \tag{22}$$

For example, near equilibrium, the viscosity η_0 is extracted using the standard Kubo formula with the perturbation $B_0 \sim e^{-i\omega t}$ by taking the limit $\omega/T \ll 1$, in which case it is clear that (22) is satisfied, yielding the KSS result $\eta_0/\mathcal{S} = 1/4\pi$ in the hydrodynamic limit.

In the present case with the shear deformation of (3), $\lim_{t\to\infty} \frac{\ddot{B}_0}{\dot{B}_0} = -2$ and $\lim_{t\to\infty} \frac{\dddot{B}_0}{\dot{B}_0} = 4$.

To further illustrate condition (22), we take

$$B_0(t) = \frac{c}{(1+e^{t/\tau})^{1/N}}\,, \tag{23}$$

which follows that

$$\lim_{t\to\infty} \left| \frac{B_0^{(n)}}{\dot{B}_0} \right| = \left(\frac{1}{N} \right)^{n-1}\,. \tag{24}$$

in the condition of $\tau = 1$.

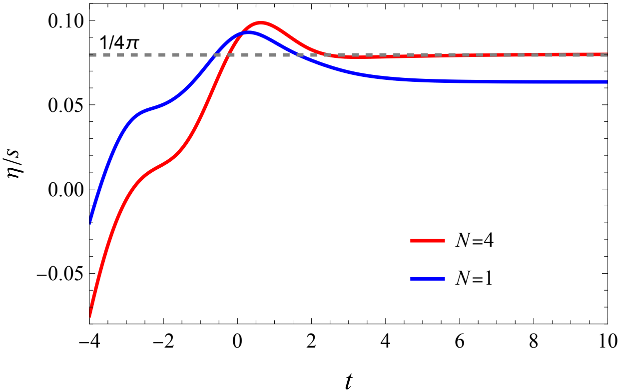

The evolution of $\eta/\mathcal{S}$ in far-from-equilibrium isotropization for the new quench function (23). The red line is for $N = 4$, and the blue one is for $N = 1$. The former case saturates at a value very close to $1/4\pi$ while for the latter $\eta/\mathcal{S} \approx 0.063$ at late times. We choose a small value of initial energy density with $c = 2$.

Conclusions

- We have investigated the isotropization dynamics of supersymmetric Yang-Mills plasma in far-from-equilibrium scenarios, demonstrating rapid isotropization, consistent with estimates from RHIC heavy-ion collisions.
- The isotropization time depends on both the strength of the applied quench and the system's initial energy density. The large initial energy densities significantly accelerate the isotropization.
- The late-time equilibrium value of $\eta/\mathcal{S}$ is generally less than the KSS bound, $\eta_0/\mathcal{S} = 1/4\pi$. Nevertheless, the value of such equilibrium ratio increases as both the strength of quench and initial energy density (or equivalently T_{eq}) are increased, approaching the KSS bound $1/4\pi$ from below.
- The equilibrium value of $\eta/\mathcal{S}$ should depend on the driven function. In particular, in cases where higher derivative terms are negligible at late times, one will recover the KSS result.

Thanks For Your Attention! Any questions?